

Special Issue

Octahedral Hexachloro Environment of Dy³⁺ with Slow Magnetic Relaxation and Luminescent Properties

Nesrine Benamara,^[a, b] Mayoro Diop,^[a] Cédric Leuvrey,^[a] Marc Lenertz,^[a] Pierre Gilliot,^[a] Mathieu Gallart,^[a] Hélène Bolvin,^[c] Fatima Setifi,^[b] Guillaume Rogez,^[a] Pierre Rabu,^[a] and Emilie Delahaye^{*[a, d]}

The compound [BiCNIm]₃[DyCl₆] was synthesized from a nitrile-functionalized imidazolium ionic liquid [BiCNIm][Cl] and DyCl₃·6H₂O in acetonitrile using solvothermal conditions. Structural characterization reveals that the Dy³⁺ ions are in a quasi-regular octahedral environment, formed by six chloride

anions. The magnetic study indicates that this mononuclear compound exhibits a Single Ion Magnet behaviour. This behaviour is compared to that of other mononuclear compounds containing Dy³⁺ ions in various octahedral environment.

Introduction

Since the pioneering works on [Mn₁₂O₁₂(CH₃CO₂)₁₆(H₂O)₄],^[1] different synthetic strategies have been elaborated to obtain compounds with efficient Single Molecule Magnet (SMM) behaviours, *i.e.* usable as ultra-small magnetic bit for high-density data storage, integrated component for spintronics or Qbits for quantum applications.^[2–11] The use of SMM for such applications is strongly hampered by the low temperature necessary for stabilizing the SMM state^[7] as well as low chemical stability, especially when integrated onto surfaces,^[12–15] or disentanglement/decoherence problem.^[16–19] Many efforts have initially concerned the elaboration of molecular compounds of high nuclearity to maximize the total spin moment of the system, combined with high anisotropy barrier. Despite many interesting achievements,^[20–24] the approach was much limited due to the difficulty for maintaining the local anisotropy of each magnetic centre in a particular direction and fully controlling the magnetic exchange pathways within the polynuclear entities. More recently, the possibility to build SMMs involving only one magnetic ion exhibiting high

anisotropy, also called Single Ion Magnet (SIM), has been explored. In particular, the pioneering works on bis(phthalocyaninato)-lanthanide complexes have largely contributed to the success of this approach.^[25,26] Since then, different ligands were synthesized to tailor the coordination sphere around the lanthanide ion, giving the possibility to establish magneto-structural correlations, especially concerning the symmetries of the ligand field around the magnetic centre (C_{∞v}, D_{5h}, D_{4d}, C_{3v},...^[27–34] Nevertheless, difficulties to reach certain symmetries remain, principally related to the fact that lanthanide ions tends to present high coordination numbers. Regarding SIMs, only few examples of mononuclear compounds containing lanthanide ions in octahedral environment were reported.^[35–45]

Possibility to achieve unusual coordination environments for Ln³⁺ ions was observed with the use of Ionic Liquids (ILs).^[46] In particular, the formation and stabilization of octahedral entities of formula [LnCl₆]^{3–} in the solid state was described using phosphonium or alkyl imidazolium ILs with Ln chloride salts.^[47–49] However, no information on possible slow relaxation of the magnetization was reported for these compounds.

This article describes the synthesis and the characterization of the compound [BiCNIm]₃[DyCl₆] obtained in solvothermal conditions by reacting DyCl₃·6H₂O with the 1,3-bis((cyanomethyl)imidazolium) chloride IL [BiCNIm][Cl]. [BiCNIm]₃[DyCl₆] is constituted of quasi-regular octahedral [DyCl₆]^{3–} entities surrounded by imidazolium cations [BiCNIm]⁺. The magnetic properties have been analyzed evidencing a SIM behaviour for the Dy³⁺ ions in this environment. The detailed analysis of the properties suggests a combination of Raman, Orbach and Quantum Tunneling (QTM) relaxation mechanisms. Luminescent properties at room temperature for this compound are also reported.

[a] Dr. N. Benamara, Dr. M. Diop, C. Leuvrey, Dr. M. Lenertz, Dr. P. Gilliot, Dr. M. Gallart, Dr. G. Rogez, Dr. P. Rabu, Dr. E. Delahaye
Institut de Physique et Chimie des Matériaux de Strasbourg – UMR 7504
Université de Strasbourg and CNRS
67034 Strasbourg, France
E-mail: emilie.delahaye@lcc-toulouse.fr

[b] Dr. N. Benamara, Dr. F. Setifi
Laboratoire de Chimie, Ingénierie Moléculaire et Nanostructures
Université Ferhat Abbas Sétif 1
Sétif 19000, Algeria

[c] Dr. H. Bolvin
Laboratoire de Chimie et de Physique Quantiques
Université de Toulouse and CNRS
31062 Toulouse, France

[d] Dr. E. Delahaye
Laboratoire de Chimie de Coordination
Université de Toulouse and CNRS
31077 Toulouse, France

Supporting information for this article is available on the WWW under <https://doi.org/10.1002/ejic.202100143>

Part of the joint "ECPM Strasbourg Institute Feature" Collection with EurJOC.



Nesrine Benamara earned her master 1 of environmental chemistry in 2014 from the University of Setif (Algeria) and her master 2 of analytical chemistry in 2015 from the University of Strasbourg (France). In 2020, she obtained her PhD from the University of Strasbourg (at the Institute of Physics and Chemistry of Materials of Strasbourg) and the University of Setif (at the Laboratoire de Chimie, Ingénierie Moléculaire et Nanostructure) under the supervision of Dr. P. Rabu, Prof. F. Setifi and Dr. E. Delahaye. During her PhD, she worked on the synthesis of new magnetic and luminescent networks using functional ligands based on imidazolium salts or triazole derivatives.



Mayoro DIOP is titular Professor of Coordination, Analytical and Environmental Chemistry at the University Cheikh Anta Diop of Dakar (Senegal), General Inspector of Education and Training in Physical Sciences and member of Division II Inorganic Chemistry of the International Union of Pure and Applied Chemistry (IUPAC).



Cédric Leuvre has a position of engineer on the MEB-Cro platform of the Institute of Physique and Chemistry of Materials of Strasbourg since 2001 and works on the characterization of materials by Scanning Electron Microscopy and EDX analysis.



Marc LENERTZ did his PhD at the Institute of Physique and Chemistry of materials (IPCMS: University of Strasbourg – CNRS) under the supervision of Silviu COLIS in the field of the structural and magnetic properties of oxides thin films. Then he got a Postdoctoral position at the Laboratoire Léon Brillouin (LLB: CEA) and was working on neutron diffraction. Since 2015, he got a position as engineer and head of the X-Ray diffraction platform of the IPCMS back in Strasbourg.



Pierre Gilliot is "Research Director" at the CNRS. He was born in 1964. He obtained his Ph.D. at the Louis Pasteur University of Strasbourg in 1989. From 1990 to 1991, he worked as a post-doc in the group of Prof. Hartmut Haug at the Institut für Theoretische Physik of the Frankfurt-am-Main University, in Germany. He received his habilitation in 2003. Since 1992, he has been CNRS researcher. He is the head of the team "Ultrafast spectroscopy of semiconductors" at the "Institut de Physique et Chimie des Matériaux de Strasbourg" UMR 7504 CNRS.



Mathieu GALLART – 47 years old – UDS assistant professor. After a Phd (1998–2001) dedicated to time resolved spectroscopy of nitride quantum wells (Université Montpellier 2), M. Gallart worked as postdoctoral researcher in Laboratoire de Photonique et nanostructures (Marcoussis, UPR 20) where he studied single photon sources. In 2002, he was appointed to the Université de Strasbourg as an assistant professor. His field of expertise addresses semiconductor ultra-fast spectroscopy including spin and phase relaxation dynamics. The publications co-authored by M. Gallart have been cited more than 1400 times; 21 of them have been cited more than 21 time (h factor of 21 according to web of science).



Hélène Bolvin earned her M.Sc. degree in Chemistry from ENS Saint-Cloud-Lyon (France) and received her Ph.D. degree in 1993 from Université Paris-Sud (France), under the supervision of Prof. Olivier Kahn. She is senior CNRS researcher in Toulouse (France) with subsequent positions in Tromsø (Norway) and Strasbourg (France). Her research interests focus on the quantum chemistry description of magnetic properties of f complexes.



Guillaume Rogez graduated from Ecole Normale Supérieure de Cachan in 1999. He obtained his PhD from the University of Paris-Sud Orsay (now Paris Saclay) under the supervision of Pr. Talal Mallah, working in coordination chemistry and molecular magnetism. He was then a post-doctoral fellow in the Department of Chemistry of the University of Bologna, under the supervision of Pr. Vincenzo Balzani, Pr. Alberto Credi and Pr. Maria-Teresa Gandolfi, working on the photochemical properties of supramolecular assemblies. He entered the CNRS in the Institute of Physics and Chemistry of Materials of Strasbourg, working on layered hybrid materials (hydroxides and oxides) and on their controlled exfoliation for magnetic and optical applications, and more recently for CO₂ electroreduction.



Fatima SETIFI graduated from the university of Constantine 1 in Algeria and received her PhD from the university of Rennes1 in France. Then, she held a Postdoctoral position at the University of Brest in the field of switchable materials. She works currently as a Professor at the university of Ferhat Abbas-Setif 1 in Algeria. Her research work is mainly located in the field of molecular chemistry including design and synthesis. It covers certain aspects of material sciences, such as magnetic, switchable and luminescent materials. She published more than 70 papers. Her h-index is 21 with more than 1061 citations.



Pierre Rabu was born in Nantes, France, in 1964. He obtained his PhD in solid state chemistry from the University of Nantes, France, in 1990. He then became CNRS researcher at the Institute of Physics and chemistry of Strasbourg, IPCMS, France, to work on low-dimensional (LD) magnetic materials. He works in the Department of Chemistry of Inorganic Materials, which is a joint department with the European School of Chemistry, Polymers and Materials of Strasbourg (ECPM). He was short term research fellow at Institute for Fundamental Organic Chemistry, Kyushu University, Fukuoka, Japan, in 1996 and visiting fellow of Advanced Materials Research Institute, University of New Orleans, USA, in 2001. He received the 1998 prize of the Solid State Chemistry division of the French Chemical Society. Since 2005, Pierre Rabu is director of research and focuses his activities on the design of molecular, inorganic or hybrid organic-inorganic solids, with a special emphasis on synthesis, structure-properties relationships, modeling and analysis of the magnetic behaviour of LD systems. His current activities involve especially layered materials, multifunctional hybrid materials and magnetic, photo active, or chiral 3d or 4f metal-based inorganic structures. In 2005–2008, he was director of the CNRS national group of research on Multifunctional Hybrid Materials. Pierre Rabu was head of the Department of Chemistry of Inorganic Materials (2014–2017) and is director of IPCMS since 2018.



Emilie Delahaye obtained her PhD in 2007 from the University of Paris-Sud Orsay under the supervision of Pr. René Clément working on the synthesis of nanoparticles exhibiting nonlinear optical properties. From 2007 to 2012, she held various post-doctoral fellows working first on the synthesis of multifunctional lamellar compounds (at the Institute of Physics and Chemistry of Materials of Strasbourg with Dr. G. Rogez and Dr. P. Rabu and then to the Max Planck Institute of Mainz with Dr. A. Taubert and Pr. J. Gütmann) and then on the synthesis of magnetic and photomagnetic nanoparticles (at the University of Paris-Sud Orsay with Pr. A. Bleuzen). In 2012, she obtained a CNRS position at IPCMS and moved in 2018 to the Laboratory of Coordination Chemistry in Toulouse. Since 2012, she works on the synthesis of multiferroic coordination compounds (coordination networks and molecular magnets).

Results and Discussion

Synthesis

[BiCNIm]₃[DyCl₆] has been synthesized in solvothermal conditions by reacting one equivalent of DyCl₃·6H₂O with two equivalents of the nitrile-functionalized IL [BiCNIm][Cl] in acetonitrile at 363 K for 2 days. After cooling down to room temperature, colorless crystals has been obtained.

It is worth to underline here that despite the final IL/Dy stoichiometry of 3/1, only the use of 50% excess of Dy (stoichiometry 2/1) provides the crystallization of [BiCNIm]₃[DyCl₆]. Several attempts to use other solvents (water or ethanol for instance) or to change the stoichiometry of the starting mixture did not lead to the title compound. In particular, starting with a 3/1 stoichiometry as observed in the title compound, or with a larger excess of Dy (200% excess, stoichiometry 1/1) resulted only in solutions, with no formation of any crystalline compound upon further crystallization attempts.

Crystal structure of [BiCNIm]₃[DyCl₆]

[BiCNIm]₃[DyCl₆] crystallizes in the orthorhombic space group *Pbcn*. Selected crystallographic data for this compound are collected in Table S1.

The asymmetric unit consists in one Dy³⁺ ions positioned on 2-fold axis, three chloride anions coordinated to the Dy³⁺ ions and one and a half independent cations [BiCNIm]⁺ (Figure S1). The repetition of this unit in the periodic structure, gives rise to [DyCl₆]³⁻ entities aligned along the *a* axis and surrounded by [BiCNIm]⁺ cations (Figure 1).

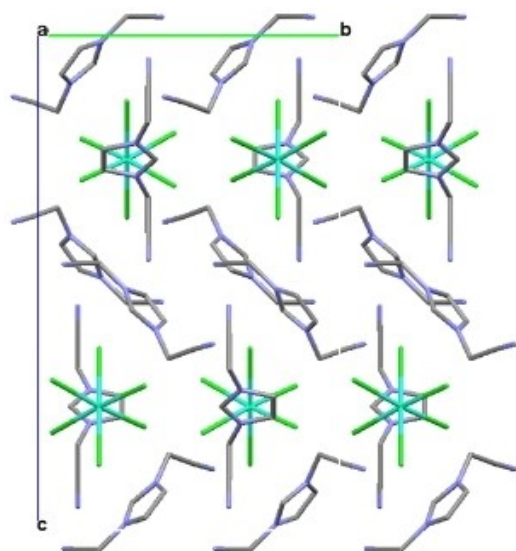


Figure 1. View showing the alternation of the cationic and anionic entities in [BiCNIm]₃[DyCl₆] along the *a* axis (Dy in cyan, Cl in green, C in grey, N in blue, H are omitted for clarity).

The Continuous Shape Measures performed with the software SHAPE^[50] showed that the coordination sphere around the Dy³⁺ ion is a quasi-regular octahedron (Table S2). The Dy–Cl distances range between 2.630(1) Å and 2.645(1) Å (Figure 2 and Table S3). These values are similar to those reported in related hexachloro compounds.^[48] The four *cis* angles Cl1–Dy–Cl1_i, Cl1_i–Dy–Cl3, Cl3–Dy–Cl3_i and Cl3_i–Dy–Cl1 are comprised between 89.19(4)° and 93.08(6)° while the *trans* angle Cl2–Dy–Cl2_i is equal to 179.95(5)° (Figure 2 and Table S3). The shortest distance between two adjacent Dy³⁺ ions is 8.9 Å.

Short interactions between chloride anions and hydrogens of the imidazolium moieties are responsible of the cohesion of the crystal (see Figure S2 and Table S4).

The phase purity of the compound obtained as crystalline powder has been investigated performing a Rietveld refinement on the powder X-ray diffraction (PXRD) pattern with the Fullprof software.^[51] It was observed that the crystal structure determined from the single crystal analysis is in agreement with the PXRD pattern (Figure S3). This study also revealed some additional peaks with low intensity (see purple arrows on Figure S3). These peaks have been attributed to the presence of a second phase likely stemming from the partial hydrolysis of the [DyCl₆]³⁻ entities as already observed in related compounds.^[49] However, as confirmed by elemental analysis and thermogravimetric analysis (Figure S4 and Figure S5), this second phase is a very minority phase and does not hamper the analysis of physical properties reported below since the decomposition product does not contribute to any of these properties. Actually, when it is left in air for few days, the compound turns to an amorphous powder (Figure S6) which is no longer luminescent and does not exhibit slow magnetic relaxation properties.

Analysis of the luminescent properties

The luminescent properties of the title compound [BiCNIm]₃[DyCl₆] have been investigated in the solid state at room temperature (Figure 3, Figure S7 and Figure S8). Under excita-

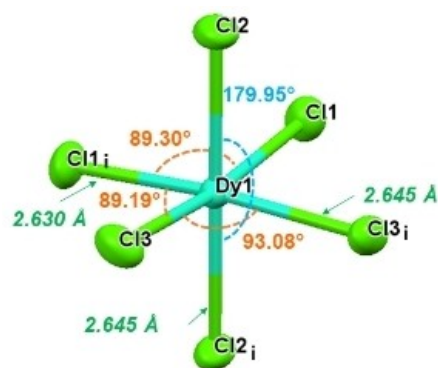


Figure 2. View in ellipsoid mode showing some selected Dy–Cl distances and Cl–Dy–Cl angles in the octahedral [DyCl₆]³⁻ entities contained in [BiCNIm]₃[DyCl₆]. Symmetry code: (i) 1–*x*, *y*, 1/2–*z*.

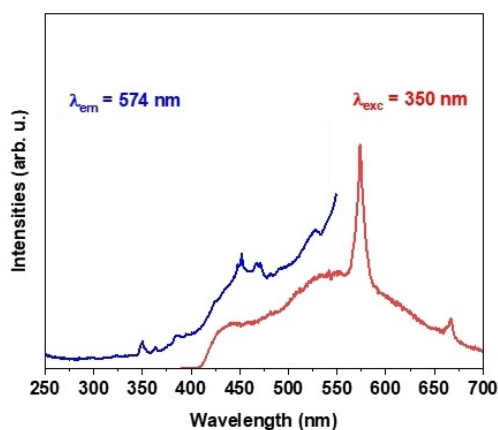


Figure 3. Photoluminescence spectrum (red line) and photoluminescence excitation spectrum (blue line) at room temperature and in solid state for $[\text{BiCNiM}]_3[\text{DyCl}_6]$.

tion at 350 nm, the emission spectrum displays a very broad band centered at 550 nm corresponding to the luminescence of the ligand (Figure S9) superimposed with two peaks centered at 574 nm and 668 nm. These two peaks are assigned to the ${}^4\text{F}_{9/2} \rightarrow {}^6\text{H}_{13/2}$ and ${}^4\text{F}_{9/2} \rightarrow {}^6\text{H}_{11/2}$ transitions of Dy^{3+} ion, respectively.^[52] The intense band at 574 nm is responsible of the yellow emission color of the compound. The peak expected for the ${}^4\text{F}_{9/2} \rightarrow {}^6\text{H}_{15/2}$ transition of Dy^{3+} ion, which is responsible for blue emission color (around 480 nm), is not observed here. Actually, this feature is merely masked by the relatively intense signal of the ligand in comparison with the one coming from the lanthanide it-self.

In the excitation spectrum, monitoring the most intense transition at 574 nm, we observe five bands at 350, 363, 385, 451 and 471 nm which can be ascribed to the transitions between the ground state ${}^6\text{H}_{15/2}$ and excited states ${}^4\text{M}_{15/2} + {}^6\text{P}_{7/2}$, ${}^4\text{I}_{11/2}$, ${}^4\text{M}_{21/2} + {}^4\text{I}_{13/2} + {}^4\text{K}_{17/2} + {}^4\text{F}_{7/2}$, ${}^4\text{I}_{15/2}$, and ${}^4\text{F}_{9/2}$ of Dy^{3+} ion, respectively.^[41] These bands are also in keeping with the absorption spectra (Figure S10).

Magnetic study

The static susceptibility measurement was performed in the 1.8–300 K temperature range with an applied field of 5000 Oe (Figure 4). The χT value at room temperature ($13.2 \text{ emu} \cdot \text{K} \cdot \text{mol}^{-1}$) is in good agreement with the expected value of $14.17 \text{ emu} \cdot \text{K} \cdot \text{mol}^{-1}$ for mononuclear Dy^{III} ion ($S = 5/2$, $L = 5$, ${}^6\text{H}_{15/2}$, $g = 4/3$).^[53] Upon cooling, the χT product decreases, because of a combination of thermal depopulation of excited M_J sublevels and significant magnetic anisotropy. Magnetization is not saturated even at 7 T because of strong magnetic anisotropy (Figure S11).

Under zero *dc* field and at 1.8 K, no out-of-phase signal is observed in the *ac* frequency range investigated, merely due to Quantum Tunneling of Magnetization (QTM).^[11] Further measurements were carried out under a small *dc* field. The optimum

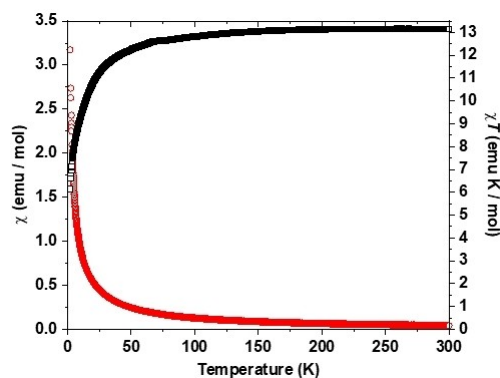


Figure 4. χT vs. T (black squares) and χ vs. T (red circles) for $[\text{BiCNiM}]_3[\text{DyCl}_6]$ under a static *dc* field of 5000 Oe.

field value to reduce QTM was chosen as the one that provides the slowest magnetic relaxation (Figure S12a and Figure S12b), *i.e.* 500 Oe. It can be seen on Figure S12a, there are (at least) two relaxations modes, one at high frequency in low fields (between 100 and 1000 Oe), and another one at low frequencies, which appears when the applied *dc* field increases.

Finally, *ac* susceptibility measurements were performed as a function of the *ac* field frequency between 1.8 K and 3.86 K under this optimized *dc* field of 500 Oe determined above (Figure S13 and Figure 5).

Figure S14 shows the corresponding Cole-Cole plot. It appears clearly on this plot, but also on the $\chi' = f(\nu)$ and $\chi'' = f(\nu)$, that the distribution of the relaxation times for this compound is non-symmetrical. Therefore, a generalized Debye model is unable to fit properly the *ac* data (Figure S15).^[54,55] This asymmetry of the relaxation time distribution at 500 Oe can be due to the vicinity of different relaxation modes, difficult to discriminate or to some structural disorder.

The relaxation times were determined from the maxima of the $\chi'' = f(\nu)$ curves (Table S5). These τ values are consistent with those usually encountered for other SIMs.^[56–58] The plot of the

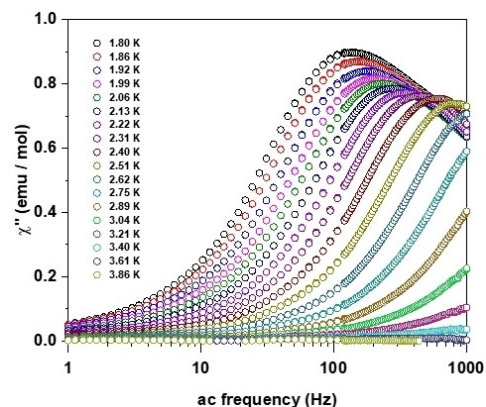


Figure 5. Out-of-phase susceptibility curves for $[\text{BiCNiM}]_3[\text{DyCl}_6]$ measured with an *ac* field of 10 Oe for $10 \text{ Hz} < \nu < 120 \text{ Hz}$ and 2 Oe for $120 \text{ Hz} < \nu < 1000 \text{ Hz}$ under a static *dc* field of 500 Oe at various temperatures.

relaxation time as a function of temperature can be equally well fitted by a Raman+QTM process ($\tau^{-1} = \tau_{QTM}^{-1} + C \times T^n$ with $\tau_{QTM} = 1.8(4) \cdot 10^{-3}$ s, $C = 3(2)$ s⁻¹·K⁻ⁿ and $n = 7.9(6)$) or by an Orbach+QTM process ($\tau^{-1} = \tau_{QTM}^{-1} + \tau_0^{-1} e^{-U_{eff}/T}$ with $\tau_{QTM} = 1.4(2) \cdot 10^{-3}$ s, $\tau_0 = 9(5) \cdot 10^{-8}$ s and $U_{eff} = 20(2)$ K⁻¹) (Figure 6). The values of the parameters are within the range of values determined for other Dy³⁺ SIMS in octahedral environment (Table 1). Even though n should be equal to 9 for a Kramers ion, it can take lower values, down to n = 4.^[59–62]

Distinction between Raman and Orbach mechanisms is here rather difficult as the fits are equally good. Due to the very limited temperature range, a fit considering both Orbach and Raman mechanisms is clearly overparametrized. Therefore, the fits were performed considering the two mechanisms separately, along with remaining QTM mechanism, which is not totally suppressed by application of a dc field. Nevertheless, the three mechanisms likely coexist in this temperature range,

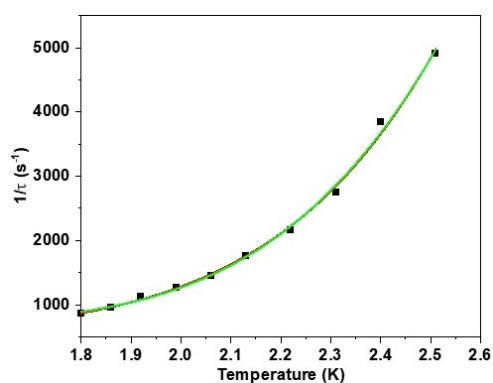


Figure 6. Inverse of the relaxation time as a function of T (black squares: experimental points, full red line: best fit using Raman + QTM process, full green line: best fit using Orbach + QTM process).

which is also suggested by the asymmetric distribution of the relaxation rates.

In order to have further insight in the magnetic behaviour, we have examined the structures of compounds showing Dy³⁺ ions in different octahedral environments (Figure 7 and Table S6) and some characteristic values describing their magnetic behaviours are given in Table 1.^[35–43] Since the local geometry influences the magnetic properties, we have limited this research to compounds containing Dy³⁺ ions surrounded by six ligands in an octahedral geometry (see CShM values in Table 1). As one can observe, the majority of these compounds showing SIM properties tends to exhibit the shorter distances along the axial direction and angle values comprised between 170° and 180°. When the compounds exhibit an equatorial crystal field with the four shortest distances in the equatorial plane (see for example third line in Figure 7), almost no compound exhibits SIM behaviour. Beyond consideration of the local symmetry, it seems that coordination of halides with decreasing electronegativity in the equatorial plane generates increasing values of U_{eff} (i.e. longer bond length and weaker ligand field, see for example first line in Figure 7). These observations are in agreement with the assumption that oblate electron densities would be more efficient for SIM properties with axial ligand fields.^[5,4,63]

Concerning the nature of the mechanisms involved in the relaxation of the magnetization for these compounds, it can be noticed that QTM mechanism is not suppressed and that Orbach and Raman processes are both suggested in numerous cases.

Theoretical study

To probe the electronic structure and the magnetic anisotropy of the title compound **[BiCNlm]₃[DyCl₆]**, *ab initio* calculations

Table 1. Nature of atoms constituting the first coordination sphere, values of the deviation from an ideal octahedron, relaxation time for QTM (τ_{QTM}), effective energy barrier (U_{eff}), relaxation rate (τ_0), values of n and C for Raman process, additional dc field used for the ac measurements of different mononuclear compounds containing Dy³⁺ ions in octahedral environment.

Compound	Sphere	CShM ^[a]	τ_{QTM} [s]	U_{eff} [K]	τ_0 [s]	n	C [s ⁻¹ ·K ⁻ⁿ]	H_{dc} [Oe]	Ref
[DyI ₃ (Cy ₃ PO) ₂ (CH ₃ CN)]	DyO ₂ N ₁ I ₃	2.57	4.7×10^{-3}	1002	5.0×10^{-12}	2.95	0.017	0	41
[DyI ₃ (Cy ₃ PO) ₃] · 2THF	DyO ₃ I ₃	2.85	0.44×10^{-3}	–	–	3.67	0.11	0	41
[DyBr ₃ (OPPh ₃) ₂ (THF)] · THF	DyO ₃ Br ₃	1.40	0.02	70.9	1.6×10^{-6}	4.3	0.0002	400	39
[DyCl ₃ (OPPh ₃) ₂ (THF)] · THF	DyO ₃ Cl ₃	0.85	0.05	49.1	2.0×10^{-6}	6.4	0.003	400	39
[DyCl ₃ (OPPh ₃) ₃] · 0.5((CH ₃) ₂ CO)	DyO ₃ Cl ₃	0.63	0.045	35.1	1.31×10^{-5}	8.0	0.058	1000	37
[DyCl ₂ (Im ^{DiPPN})(THF) ₃]	DyO ₃ N ₁ Cl ₂	0.96	–	803	1.4×10^{-12}	4.0	0.00086	0	38
[DyCl ₂ (OAr*)(THF) ₃]	DyO ₄ Cl ₂	0.97	3.19×10^{-4}	52	8.0×10^{-6}	4.64	0.018	0	38
[DyR ₂ (THF) ₄][BPh ₄]	DyO ₄ N ₂	0.16	0.76×10^{-3}	57.6	2.0×10^{-5}	5 ^[b]	0.00005	0	42
[DyR ₂ (py) ₄][BPh ₄] · 2py	DyN ₆	0.11	4.6×10^{-3}	72.0	7×10^{-5}	5 ^[b]	0.0000083	0	42
[Dy(TpMe ₂) ₂]I	DyN ₆	1.57	–	13.5	1.6×10^{-6}	6	0.1	800	35
[DyCl ₂ (H ₂ NAP) ₂]Cl · EtOH	DyO ₄ Cl ₂	1.16	24×10^{-3}	22.9	2.9×10^{-6}	2.7	3.2	1200	40
[DyCl ₂ (Ph ₃ AsO) ₄]Cl · Solv	DyO ₄ Cl ₂	0.87	–	–	–	–	–	–	43
[DyCl ₂ (OPPh ₃) ₄]Cl · solv	DyO ₄ Cl ₂	0.60	–	–	–	–	–	–	37
[DyI ₂ (OPPh ₃) ₄] · 4THF · 0.3H ₂ O	DyO ₄ I ₂	2.50	–	–	–	–	–	–	39
[BiCNlm] ₃ [DyCl ₆] ^[c]	DyCl ₆	0.25	1.8×10^{-3}	–	–	7.9	3	500	This work
[BiCNlm] ₃ [DyCl ₆] ^[d]	DyCl ₆	0.25	1.4×10^{-3}	20	9×10^{-8}	–	–	500	This work
[Dy(L ²) ₂]	DyO ₂ N ₄	1.70	–	–	–	–	–	–	36
(NMe ₄)[DyCl ₃ (Tp ^{Me2}) ₂]	DyO ₃ Cl ₃	1.70	–	–	–	–	–	–	35

[a] Minimal value determined for OC-6 or Oh geometry from the CShM calculation. [b] Fixed value during the fit of the data. [c] Values determined from the fit using Raman + QTM process. [d] Values determined from the fit using Orbach + QTM process.

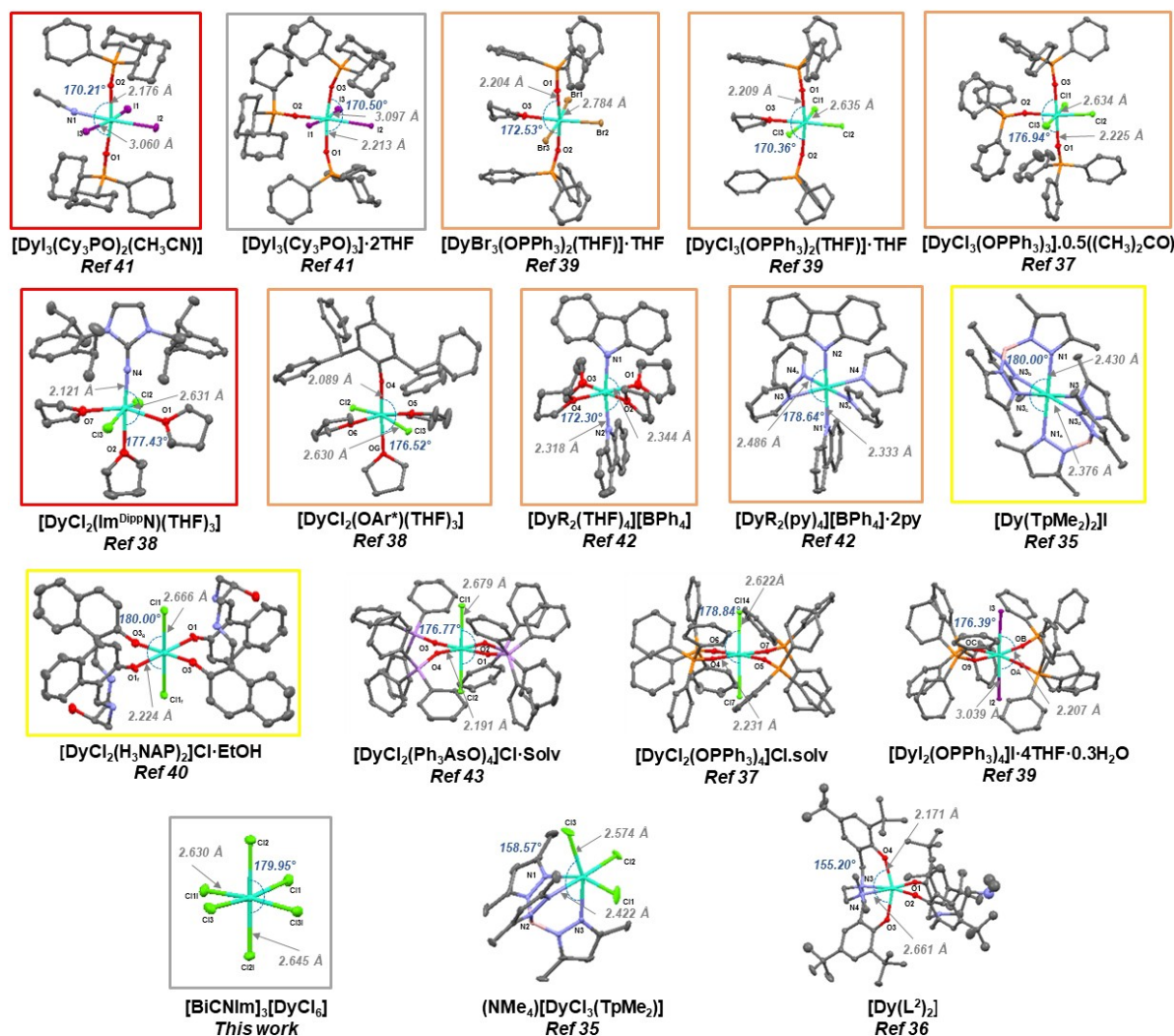


Figure 7. Representation of different octahedral environments observed in mononuclear Dy³⁺ based compounds (dysprosium in cyan, carbon in grey, oxygen in red, nitrogen in blue, phosphorus in orange, chloride in green, bromide in brown, iodide in violet, boron in pink). Values of shorter and longer distances as well as axial angle have been indicated on this figure (for more details, see Table S6). Coloured frames indicate the compounds for which the SIM behaviour has been observed and their colour is related to the values of U_{eff} : red for large values of U_{eff} , yellow for small U_{eff} and orange for intermediate U_{eff} . Grey box corresponds to the title compound exhibiting equivalent Raman + QTM mechanisms and Orbach + QTM mechanisms (see Table 1).

have been performed using the SO-CASSCF method. It has been shown for octahedral f complexes that the ligand field can be written as following:^[64]

$$\hat{V}_{CF} = W \left[x \frac{\hat{O}_4}{F(4)} + (1 - |x|) \frac{\hat{O}_6}{F(6)} \right] \quad (1)$$

with $\hat{O}_4 = \hat{O}_4^0(J) + 5\hat{O}_4^4(J)$ and $\hat{O}_6 = \hat{O}_6^0(J) - 215\hat{O}_6^4(J)$, $\hat{O}_k^q(J)$ are the Stevens operators for the J manifold, $F(4)$ and $F(6)$ are factors dependent of the J value, x and W are two adjustable parameters, W defining the energy scale and x the ratio between the fourth and the sixth orders. To understand the influence of the symmetry, the SO-CASSCF calculations have been realized considering first an idealized case formed by a

symmetrized $[\text{DyCl}_6]^{3-}$ octahedral structure and then the X-ray structure. Details for these calculations are reported in computational details and in SI part. Figure 8 gives the calculated *ab initio* energies and the corresponding g factors for the symmetrized and crystal structures. The splitting of the ground J manifold is about 300 cm⁻¹. In the symmetrized structure, the ground state is an isotropic Kramers doublet with a g factor of 6.62 (Figure 8). The first excited quartet lies at 21 cm⁻¹ and then a Kramers doublet at 98 cm⁻¹. This ordering of the states corresponds to Eq. 1 with negative W and x . Only the crystal field parameters B_0^4 , B_4^4 , B_0^6 and B_4^6 do not vanish (Table S7). The parameter S allows to evaluate the strength of the ligand field with only one parameter. The 4th order parameter S^4 is larger than the 6th order one S^6 (Table S7), in accordance with the ordering states which implies that $|x| > 0.5$. In the crystal structure, the presence of the $[\text{BilmCN}]^+$

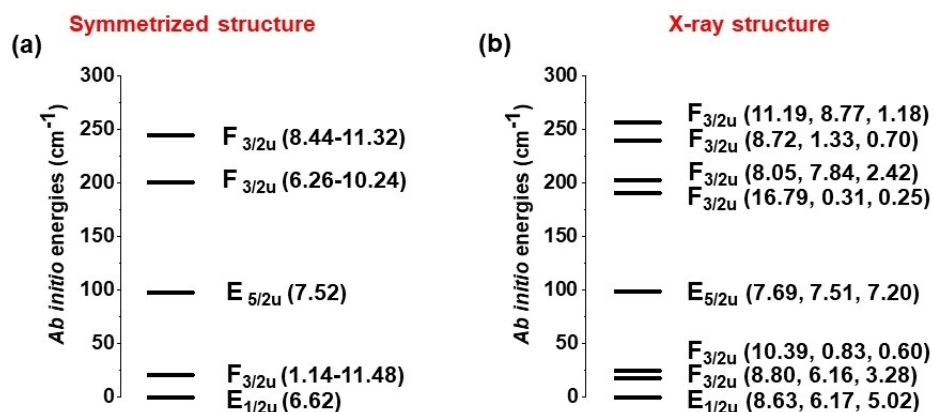


Figure 8. SO-CASSCF energies of the low-lying states and corresponding g-tensor values (in bracket) calculated (a) for the symmetrized [DyCl₆]³⁻ structure and (b) for the X-ray structure of [BiCNim]₃[DyCl₆].

cation leads to a deformation of the coordination sphere. Consequently, the quartets split into two Kramers doublets by 10 cm⁻¹ and the g tensors are anisotropic. As an example, g values of the ground Kramers doublet range from 5 to 8.6 (Figure 8). With the lowering of the symmetry, all crystal field parameters are non-zero (Table S8), but this barely affects the strength parameters and the response to the magnetic field (magnetic susceptibility). Consequently, the departure from the ideal octahedral symmetry leads to a small anisotropy in the g tensor of the ground state which can be at the origin of the SIM behaviour. This slight deviation from the ideal octahedral symmetry can also explain the absence of zero-field SIM behaviour and the probability of QTM process.

These observations tend also to indicate that existence of axiality within these octahedral Dy³⁺ based compounds is not necessary to promote SIM properties since the Dy³⁺ based compound with a more regular octahedral environment give rise to these properties. From this point of view, the possibility to access to new other compounds with more regular geometry and to explore their magnetic behaviour is particularly appealing.

Conclusion

We have reported the synthesis and the characterization of a new compound containing Dy³⁺ ions in an unusual octahedral hexachloride environment. Despite its sensitivity to air, we have been able to investigate its photoluminescent and magnetic properties. The analysis of the experimental magnetic features indicates that [BiCNim]₃[DyCl₆] exhibits SIM properties for which the relaxation mechanism involves Raman, Orbach and QTM mechanisms. In contrast with previous examples where sophisticated ligands are employed to generate an octahedral environment, this work illustrates the possibility offered by imidazolium ionic liquid to stabilize octahedral [DyCl₆]³⁻ units. This result paves the way to the synthesis of new series of lanthanide based SIMs involving other lanthanide salts with the

possibility to vary the imidazolium ILs that can be modified with different substitutions of the cationic or the anionic part.

Experimental Section

Materials and general methods

Chloroacetonitrile, trimethylsilylimidazole and DyCl₃·6H₂O were purchased from Alfa Aesar. They were used as received. Elemental analyses for C, H, N were performed at the Service de Microanalyses of the Institut de Chimie de Strasbourg. NMR spectra in solution were recorded using a Bruker AVANCE 300 spectrometer. FTIR spectra were performed on a Perkin Elmer Spectrum Two UATR-FTIR spectrometer. The powder XRD patterns were collected with a Bruker D8 diffractometer using a copper Kα₁ radiation (λ = 1.540598 Å). The SEM images were obtained with a JEOL 6700F scanning electron microscope (SEM) equipped with a field emission gun (FEG), operating at 15 kV in the composition mode of the instrument. TGA-TDA experiments were performed using a TA instrument SDT Q600 (heating rates of 5 °C·min⁻¹ under air stream).

Synthesis of the 1,3-bis((cyanomethyl)imidazolium) chloride [BiCNim][Cl]

The imidazolium salt was synthesized according to protocol adapted from the literature.^[65,66] Chloroacetonitrile (1.38 mL, 22 mmol) and trimethylsilylimidazole (1.46 mL, 10 mmol) were mixed in a round bottom flask. The mixture was stirred and heated at 333 K for 24 hours. After cooling at room temperature, the brown mixture is washed with diethyl ether (3 × 10 mL). The white solid is dried under vacuum. The yield of the reaction is around 75%.

Elemental analysis for C₇H₇N₄Cl·0.25H₂O (M = 187.0 g·mol⁻¹) Found (Calc) (%): C 45.36 (44.92), H 4.01 (4.01), N 30.30 (29.95). ¹H NMR (D₂O): δ (ppm) = 7.75 (s, 2), 5.45 (s, 4). ¹³C NMR (D₂O): δ (ppm) = 138.2, 123.5, 113.4, 37.5. IR (reflectance, cm⁻¹): 3187 (m), 3136 (w), 3097 (w), 3008 (s), 2969 (m), 2899 (w), 2260 (w), 1806 (w), 1761 (w), 1684 (m), 1563 (s), 1428 (m), 1390 (s), 1345 (m), 1294 (m), 1256 (m), 1180 (s), 1110 (m), 1033 (w), 931 (m), 873 (s), 796 (s), 719 (m), 611 (s), 521 (m), 463 (w).

Synthesis of [BiCNiM]₃[DyCl₆]

[BiCNiM][Cl] (90 mg, 0.50 mmol) and DyCl₃·6H₂O (94 mg, 0.25 mmol) were introduced in 6 mL of acetonitrile. The mixture was sealed in a Teflon-lined stainless steel bomb (23 mL) and heated at 363 K for 2 days. After cooling at room temperature, colorless crystals were obtained. They were filtered and washed with ethanol. The yield of the reaction is around 33 %.

Elemental analysis for C₂₁H₂₁N₁₂Cl₆Dy₁ (*M* = 816.5 g·mol⁻¹) Found (Calc) (%): C 33.69 (33.94), H 3.01 (2.83), N 22.38 (22.63). IR (reflectance, cm⁻¹): 3365 (sh), 3129 (w), 3104 (w), 3065 (m), 2969 (m), 2924 (w), 1622 (w), 1544 (s), 1435 (w), 1396 (w), 1345 (w), 1313 (w), 1256 (w), 1212 (w), 1174 (s), 1110 (m), 1020 (w), 918 (m), 876 (w), 835 (m), 745 (s), 617 (s), 484 (sh).

Physical measurements

X-ray measurements. Single crystal X-ray diffraction measurement was carried out at room temperature using a Kappa Nonius CCD diffractometer. The diffraction intensities were collected with graphite-monochromatized Mo K α radiation (λ = 0.71073 Å). Intensity data were corrected for Lorentz-polarization and absorption factors. The structure was solved by direct methods using SIR92,^[67] and refined against *F*² by full-matrix least-squares methods using SHELXL-2018/3^[68] with anisotropic displacement parameters for all non-hydrogen atoms. All calculations were performed by using the Crystal Structure crystallographic software package WINGX.^[69] The structures were represented with Mercury.^[70] All hydrogen atoms were introduced into the calculations as a riding model with isotropic thermal parameters.

Magnetic measurements. The magnetic measurements were conducted using a Quantum Design MPMS-3 magnetometer. The static susceptibility measurements were performed in the 1.8 K–300 K temperature range with an applied field of 0.5 T. Samples were blocked in eicosane to avoid orientation under magnetic field. Magnetization measurements at different fields and at given temperature confirm the absence of ferromagnetic impurities. Data were corrected for the sample holder and eicosane and diamagnetism was estimated from Pascal constants.

Photoluminescence and photoluminescence excitation. These measurements were performed using a broad-spectrum Energetiq® EQ-99FC laser-driven light source (LDLSTM) spectrally filtered by a monochromator. The PL signal was dispersed in a spectrometer and detected by a cooled charge coupled device (CCD) camera.

Computational details

Calculations were performed using the MOLCAS-7.8 suite of software, on the [DyCl₆]³⁻ complex for the X-rays geometry and a symmetrized octahedral structure with a Dy–Cl distance of 2.64 Å. Relativistically contracted ANO-RCC basis sets of TZP quality were used.^[71,72] Firstly, a SF-CASSCF (spin-free CASSCF) calculation was performed^[73] with an active space composed of the seven 4f orbitals of the lanthanide ion and associated electrons, that is, CAS (9,7). Spin-orbit (SO) coupling was included by a state interaction with the RASSI (restricted active space state interaction) method.^[74] 21 sextets and 108 quartets were considered for the state interaction. Scalar relativistic effects were taken into account by means of the Douglas-Kroll-Hess transformation,^[75] and the SO integrals were calculated by using the AMFI (atomic mean-field integrals) approximation. *g*-values were calculated according to reference^[76] and CFPs were calculated with a local program written in Mathematica as described in references.^[77,78]

Deposition Number 2045435 (for [BiCNiM]₃[DyCl₆]) contains the supplementary crystallographic data for this paper. These data are provided free of charge by the joint Cambridge Crystallographic Data Centre and Fachinformationszentrum Karlsruhe Access Structures service www.ccdc.cam.ac.uk/structures.

Acknowledgements

The authors thank the Centre National de la Recherche Scientifique (CNRS), the Université de Strasbourg (Idex), the Labex NIE (ANR-11-LABX-0058-NIE within the Investissement d'Avenir program ANR-10-IDEX-0002-02) for funding. Nesrine Benamara thanks the program Profas B⁺ of Campus France for the grant of her PhD and the Direction Générale de la Recherche Scientifique et du Développement Technologique (DGRSDT). The authors are grateful to Didier Burger for technical assistance.

Conflict of Interest

The authors declare no conflict of interest.

Keywords: Ionic liquid · Imidazolium salt · Lanthanide · Single ion magnet · Luminescence

- [1] R. Sessoli, D. Gatteschi, A. Caneschi, M. A. Novak, *Nature* **1993**, *365*, 141–143.
- [2] T. Komeda, K. Katoh, M. Yamashita, in *Mol. Technol.*, John Wiley & Sons, Ltd, **2019**, pp. 263–304.
- [3] A. Cornia, M. Mannini, R. Sessoli, D. Gatteschi, *Eur. J. Inorg. Chem.* **2019**, *2019*, 552–568.
- [4] L. Ungur, L. F. Chibotaru, *Inorg. Chem.* **2016**, *55*, 10043–10056.
- [5] S. G. McAdams, A.-M. Ariciu, A. K. Kostopoulos, J. P. S. Walsh, F. Tuna, *Coord. Chem. Rev.* **2017**, *346*, 216–239.
- [6] H. L. C. Feltham, S. Brooker, *Coord. Chem. Rev.* **2014**, *276*, 1–33.
- [7] D. N. Woodruff, R. E. P. Winpenny, R. A. Layfield, *Chem. Rev.* **2013**, *113*, 5110–5148.
- [8] L. Bogani, W. Wernsdorfer, *Nat. Mater.* **2008**, *7*, 179–186.
- [9] A. Ardavan, O. Rival, J. J. L. Morton, S. J. Blundell, A. M. Tyryshkin, G. A. Timco, R. E. P. Winpenny, *Phys. Rev. Lett.* **2007**, *98*, 057201.
- [10] M. N. Leuenberger, D. Loss, *Nature* **2001**, *410*, 789–793.
- [11] G. Christou, D. Gatteschi, D. N. Hendrickson, R. Sessoli, *MRS Bull.* **2000**, *25*, 66–71.
- [12] D. Mitcov, A. H. Pedersen, M. Ceccato, R. M. Gelardi, T. Hassenkam, A. Konstantatos, A. Reinholdt, M. A. Sørensen, P. W. Thulstrup, M. G. Vinum, F. Wilhelm, A. Rogalev, W. Wernsdorfer, E. K. Brechin, S. Piligkos, *Chem. Sci.* **2019**, *10*, 3065–3073.
- [13] E. Kiefl, M. Mannini, K. Bernot, X. Yi, A. Amato, T. Leviant, A. Magnani, T. Prokscha, A. Suter, R. Sessoli, Z. Salman, *ACS Nano* **2016**, *10*, 5663–5669.
- [14] M. Mannini, P. Sainctavit, R. Sessoli, C. Cartier dit Moulin, F. Pineider, M.-A. Arrio, A. Cornia, D. Gatteschi, *Chem. Eur. J.* **2008**, *14*, 7530–7535.
- [15] L. Bogani, L. Cavigli, M. Gurioli, R. L. Novak, M. Mannini, A. Caneschi, F. Pineider, R. Sessoli, M. Clemente-León, E. Coronado, A. Cornia, D. Gatteschi, *Adv. Mater.* **2007**, *19*, 3906–3911.
- [16] K. Bader, D. Dengler, S. Lenz, B. Endeward, S.-D. Jiang, P. Neugebauer, J. van Slageren, *Nat. Commun.* **2014**, *5*, 5304.
- [17] A. Candini, G. Lorusso, F. Troiani, A. Ghirri, S. Carretta, P. Santini, G. Amoretti, C. Muryn, F. Tuna, G. Timco, E. J. L. McInnes, R. E. P. Winpenny, W. Wernsdorfer, M. Affronte, *Phys. Rev. Lett.* **2010**, *104*, 037203.
- [18] A. Wilson, S. Hill, R. S. Edwards, N. Aliaga-Alcalde, G. Christou, *AIP Conf. Proc.* **2006**, *850*, 1141–1142.
- [19] S. Hill, R. S. Edwards, N. Aliaga-Alcalde, G. Christou, *Science* **2003**, *302*, 1015–1018.

- [20] S.-G. Wu, Y.-Y. Peng, Y.-C. Chen, J.-L. Liu, M.-L. Tong, *Dalton Trans.* **2020**, 49, 14140–14147.
- [21] C. Zhang, X. Ma, P. Cen, X. Jin, J. Yang, Y.-Q. Zhang, J. Ferrando-Soria, E. Pardo, X. Liu, *Dalton Trans.* **2020**, 49, 14123–14132.
- [22] D. Maniaki, E. Pilichos, S. P. Perlepes, *Front. Chem.* **2018**, 6, 1–28.
- [23] K. S. Pedersen, J. Bendix, R. Clérac, *Chem. Commun.* **2014**, 50, 4396–4415.
- [24] M. Nakano, H. Oshio, *Chem. Soc. Rev.* **2011**, 40, 3239–3248.
- [25] K. Najafi, A. L. Wysocki, K. Park, S. E. Economou, E. Barnes, *J. Phys. Chem. Lett.* **2019**, 10, 7347–7355.
- [26] N. Ishikawa, M. Sugita, T. Ishikawa, S. Koshihara, Y. Kaizu, *J. Am. Chem. Soc.* **2003**, 125, 8694–8695.
- [27] A. Arauzo, L. Gasque, S. Fuertes, C. Tenorio, S. Bernès, E. Bartolomé, *Dalton Trans.* **2020**, 49, 13671–13684.
- [28] C. D. Buch, D. Mitcov, S. Piligkos, *Dalton Trans.* **2020**, 49, 13557–13565.
- [29] M. Kong, X. Feng, J. Li, Z.-B. Hu, J. Wang, X.-J. Song, Z.-Y. Jing, Y.-Q. Zhang, Y. Song, *Dalton Trans.* **2020**, 49, 14931–14940.
- [30] S. K. Gupta, R. Murugavel, *Chem. Commun.* **2018**, 54, 3685–3696.
- [31] J.-L. Liu, Y.-C. Chen, M.-L. Tong, *Chem. Soc. Rev.* **2018**, 47, 2431–2453.
- [32] M. Feng, M.-L. Tong, *Chem. Eur. J.* **2018**, 24, 7574–7594.
- [33] J. Lu, M. Guo, J. Tang, *Chem. Asian J.* **2017**, 12, 2772–2779.
- [34] G. Cucinotta, M. Perfetti, J. Luzon, M. Etienne, P.-E. Car, A. Caneschi, G. Calvez, K. Bernot, R. Sessoli, *Angew. Chem. Int. Ed.* **2012**, 51, 1606–1610; *Angew. Chem.* **2012**, 124, 1638–1642.
- [35] D. I. Alexandropoulos, K. R. Vignesh, H. Xie, K. R. Dunbar, *Dalton Trans.* **2019**, 48, 10610–10618.
- [36] M. Guo, J. Tang, *Inorganics* **2018**, 6, 16.
- [37] S. K. Langley, K. R. Vignesh, K. Holton, S. Benjamin, G. B. Hix, W. Phonsri, B. Moubarak, K. S. Murray, G. Rajaraman, *Inorganics* **2018**, 6, 61.
- [38] B.-C. Liu, N. Ge, Y.-Q. Zhai, T. Zhang, Y.-S. Ding, Y.-Z. Zheng, *Chem. Commun.* **2019**, 55, 9355–9358.
- [39] K. R. Vignesh, D. I. Alexandropoulos, H. Xie, K. R. Dunbar, *Dalton Trans.* **2020**, 49, 4694–4698.
- [40] S. Yu, Z. Chen, H. Hu, B. Li, Y. Liang, D. Liu, H. Zou, D. Yao, F. Liang, *Dalton Trans.* **2019**, 48, 16679–16686.
- [41] M. Li, H. Wu, Z. Xia, L. Ungur, D. Liu, L. F. Chibotaru, H. Ke, S. Chen, S. Gao, *Inorg. Chem.* **2020**, 59, 7158–7166.
- [42] J. Long, A. N. Selikhov, E. Mamontova, K. A. Lyssenko, Y. Guari, J. Larionova, A. A. Trifonov, *Dalton Trans.* **2020**, 49, 4039–4043.
- [43] M. Fondo, J. Corredoira-Vázquez, A. M. García-Deibe, J. Sanmartín-Matalobos, J. M. Herrera, E. Colacio, *Front. Chem.* **2018**, 6, DOI 10.3389/fchem.2018.00420.
- [44] M. Gregson, N. F. Chilton, A.-M. Ariciu, F. Tuna, I. F. Crowe, W. Lewis, A. J. Blake, D. Collison, E. J. L. McInnes, R. E. P. Winpenny, S. T. Liddle, *Chem. Sci.* **2015**, 7, 155–165.
- [45] J.-L. Liu, K. Yuan, J.-D. Leng, L. Ungur, W. Wernsdorfer, F.-S. Guo, L. F. Chibotaru, M.-L. Tong, *Inorg. Chem.* **2012**, 51, 8538–8544.
- [46] K. Binnemans, *Chem. Rev.* **2009**, 109, 4283–4374.
- [47] J. Alvarez-Vicente, S. Dandil, D. Banerjee, H. Q. N. Gunaratne, S. Gray, S. Felton, G. Srinivasan, A. M. Kaczmarek, R. Van Deun, P. Nockemann, *J. Phys. Chem. B* **2016**, 120, 5301–5311.
- [48] Y. Han, C. Lin, Q. Meng, F. Dai, A. G. Sykes, M. T. Berry, P. S. May, *Inorg. Chem.* **2014**, 53, 5494–5501.
- [49] C. C. Hines, D. B. Cordes, S. T. Griffin, S. I. Watts, V. A. Cocalia, R. D. Rogers, *New J. Chem.* **2008**, 32, 872–877.
- [50] M. Pinsky, D. Avnir, *Inorg. Chem.* **1998**, 37, 5575–5582.
- [51] J. Rodriguez-Carvajal, *Phys. Condens. Matter* **1993**, 192, 55–69.
- [52] A. B. Ruiz-Muelle, A. García-García, A. A. García-Valdivia, I. Oyarzabal, J. Cepeda, J. M. Seco, E. Colacio, A. Rodríguez-Diéguez, I. Fernández, *Dalton Trans.* **2018**, 47, 12783–12794.
- [53] C. Benelli, D. Gatteschi, *Chem. Rev.* **2002**, 102, 2369–2388.
- [54] K. S. Cole, R. H. Cole, *J. Chem. Phys.* **1941**, 9, 341–351.
- [55] D. Gatteschi, R. Sessoli, J. Villain, *Molecular Nanomagnets*, Oxford University Press, **2006**.
- [56] C. Y. Chow, H. Bolvin, V. E. Campbell, R. Guillot, J. W. Kampf, W. Wernsdorfer, F. Gendron, J. Autschbach, V. L. Pecoraro, T. Mallah, *Chem. Sci.* **2015**, 6, 4148–4159.
- [57] V. E. Campbell, R. Guillot, E. Riviere, P.-T. Brun, W. Wernsdorfer, T. Mallah, *Inorg. Chem.* **2013**, 52, 5194–5200.
- [58] A. Baniodeh, Y. Lan, G. Novitchi, V. Mereacre, A. Sukhanov, M. Ferbinteanu, V. Voronkova, C. E. Anson, A. K. Powell, *Dalton Trans.* **2013**, 42, 8926–8938.
- [59] F. Pointillart, J.-K. Ou-Yang, G. Fernandez Garcia, V. Montigaud, J. Flores Gonzalez, R. Marchal, L. Favereau, F. Totti, J. Crassous, O. Cador, L. Ouahab, B. Le Guennic, *Inorg. Chem.* **2019**, 58, 52–56.
- [60] K. N. Shrivastava, *Phys. Status Solidi B* **1983**, 117, 437–458.
- [61] A. Singh, K. N. Shrivastava, *Phys. Status Solidi B* **1979**, 95, 273–277.
- [62] P. L. Scott, C. D. Jeffries, *Phys. Rev.* **1962**, 127, 32–51.
- [63] J. D. Rinehart, J. R. Long, *Chem. Sci.* **2011**, 2, 2078–2085.
- [64] K. R. Lea, M. J. M. Leask, W. P. Wolf, *J. Phys. Chem. Solids* **1962**, 23, 1381–1405.
- [65] Z. Fei, D. Zhao, D. Pieraccini, W. H. Ang, T. J. Geldbach, R. Scopelliti, C. Chiappe, P. J. Dyson, *Organometallics* **2007**, 26, 1588–1598.
- [66] D. Zhao, Z. Fei, R. Scopelliti, P. J. Dyson, *Inorg. Chem.* **2004**, 43, 2197–2205.
- [67] A. Altomare, G. Cascarano, C. Giacovazzo, A. Guagliardi, M. C. Burla, G. Polidori, M. Camalli, *J. Appl. Crystallogr.* **1994**, 27, 435.
- [68] G. Sheldrick, *Acta Crystallogr. Sect. A* **2008**, 64, 112–122.
- [69] L. Farrugia, *J. Appl. Crystallogr.* **1999**, 32, 837–838.
- [70] P. R. Edgington, P. McCabe, C. F. Macrae, E. Pidcock, G. P. Shields, R. Taylor, M. Towler, J. Van De Streek, *J. Appl. Crystallogr.* **2006**, 39, 453–457.
- [71] B. O. Roos, R. Lindh, P.-Å. Malmqvist, V. Veryazov, P.-O. Widmark, *J. Phys. Chem. A* **2004**, 108, 2851–2858.
- [72] B. O. Roos, R. Lindh, P.-Å. Malmqvist, V. Veryazov, P.-O. Widmark, *Chem. Phys. Lett.* **2005**, 409, 295–299.
- [73] B. O. Roos, P. R. Taylor, P. E. M. Sigbahn, *Chem. Phys.* **1980**, 48, 157–173.
- [74] P. Å. Malmqvist, B. O. Roos, B. Schimmelpfennig, *Chem. Phys. Lett.* **2002**, 357, 230–240.
- [75] B. A. Hess, *Phys. Rev. A* **1986**, 33, 3742–3748.
- [76] H. Bolvin, *ChemPhysChem* **2006**, 7, 1575–1589.
- [77] J. Jung, M. A. Islam, V. L. Pecoraro, T. Mallah, C. Berthon, H. Bolvin, *Chem. Eur. J.* **2019**, 25, 15112–15122.
- [78] L. Ungur, L. F. Chibotaru, *Chem. Eur. J.* **2017**, 23, 3708–3718.

Manuscript received: February 16, 2021

Revised manuscript received: April 16, 2021